https://doi.org/10.5194/egusphere-2025-1735
Preprint. Discussion started: 25 April 2025

Estimating surface sulfur dioxide concentrations from satellite data: Using chemical transport models vs. machine learning

Zachary Watson[1], Can Li[2], Fei Liu[2,3], Sean W. Freeman[1], Huanxin Zhang[4], Jun Wang[4], Shan-Hu Lee[1]

[1]Department of Atmospheric and Earth Science, University of Alabama in Huntsville, Huntsville, AL 35758
[2]NASA Goddard Space Flight Center, Greenbelt, MD 20771
[3]Goddard Earth Sciences Technology and Research (GESTAR) II, Morgan State University, Baltimore, MD 21251
[4]Department of Chemical and Biochemical Engineering, Center for Global & Regional Environmental Research, and Iowa Technology Institute, The University of Iowa, Iowa City, Iowa 52240

Correspondence to: Zachary Watson (zw0033@uah.edu) and Shan-Hu Lee (shanhu.lee@uah.edu)

Abstract. Sulfur dioxide (SO_2) is an important air pollutant that contributes to negative health effects, acid rain, and aerosol formation and growth. SO_2 has been measured using ground-based air quality monitoring networks, but the routine monitoring sites are predominantly placed in urban areas, leaving large gaps in the network in less populated locations. Previous studies have used chemical transport models (CTMs) or machine learning techniques to estimate surface SO_2 concentrations from satellite vertical column densities, but no direct comparisons between the methods have been made. In this study, we estimated surface SO_2 concentrations using Ozone Monitoring Instrument (OMI) retrievals over eastern China from 2015-2018 utilizing GEOS-Chem simulations and an extreme gradient boosting machine learning model. Compared to the in situ measurements, the SO_2 concentrations estimated from the CTM method had similar spatial distributions (r = 0.58) and intra- and interannual variations but were underestimated (slope = 0.24) with a relative percent error of ~75% and had worsening performance over time. The machine learning method produced more accurate spatial distributions (r = 0.77) and temporal variations, a smaller discrepancy and bias (~30%; slope = 0.69) and relatively stable performance over time. The machine learning method performed better than the GEOS-Chem method on smaller datasets and timescales with shorter temporal averaging periods. Ultimately, both methods were useful for estimating surface SO_2 concentrations since the CTM-based method does not rely on in situ monitoring and produced more reasonable spatial distributions than the machine learning method over areas without surface monitoring data.

1 Introduction

Sulfur dioxide (SO_2) is an important air pollutant due to its effects on human health, air quality, weather, and climate. SO_2 has many anthropogenic sources such as fossil fuel combustion in power plants and ore smelters, as well as natural sources from volcanoes (Engdahl, 1973). Surface SO_2 concentrations are mainly driven by anthropogenic activity in urban areas and are known to cause cardiovascular and respiratory health impacts (Engdahl, 1973; Krzyzanowski & Wojtyniak, 1982). SO_2 readily undergoes oxidation reactions in the atmosphere to form sulfuric acid, which contributes to

https://doi.org/10.5194/egusphere-2025-1735
Preprint. Discussion started: 25 April 2025

acid rain (Seinfeld and Pandis, 2016) and participates in aerosol formation and growth (Lee et al., 2019), leading to further effects on weather and the global energy budget (NASEM, 2016).

Concentrations of SO_2 at the surface have been measured using ground-based air quality monitoring networks. Surface concentrations are measured on hourly to daily time intervals, but the sites are predominantly located in urban areas, leaving large gaps in the network elsewhere. Satellite-based instruments can measure total-column concentrations of SO_2 globally. These SO_2 vertical column densities (VCDs) are retrieved using the absorption of backscattered solar radiation in the ultraviolet wavelengths measured by a spectrometer (e.g., Krotkov et al., 2008; Levelt et al., 2006; Li et al., 2013; Li et al., 2020a; Nowlan et al., 2011; Theys et al., 2015). The VCDs are typically available over cloud-free locations over large areas on a daily basis but do not directly provide the surface concentrations. Additional tools are required to estimate the surface concentrations from the satellite-retrieved VCDs as discussed below.

The first method is to use chemical transport models (CTMs) to convert satellite VCDs into surface concentrations using simulated surface-to-VCD ratios (SVRs). This method was initially developed for estimating surface $PM_{2.5}$ from satellite-based aerosol optical depth retrievals (Liu et al., 2004) and was later applied to nitrogen dioxide (NO_2; Lamsal et al., 2008) and SO_2 (Lee et al., 2011). Lee et al. (2011) and Zhang et al. (2021) used coarse-resolution CTMs (grid spacings on the order of 100 km) to convert SO_2 VCDs from the Ozone Monitoring Instrument (OMI) into surface concentrations over North America for 2006, and China for 2005-2018, respectively. McLinden et al. (2014) and Kharol et al. (2017) used higher-resolution CTMs (grid spacing on the order of 10 km) and OMI VCDs to estimate the surface concentrations with focuses on the Canadian oil sands from 2005-2011, and North America from 2005-2015, respectively. These studies demonstrate that annual mean satellite-derived surface SO_2 concentrations accurately capture the spatial distribution from the ground-based air quality monitoring network, despite the estimated surface concentrations being generally underestimated. An advantage of the CTM method is that it is based on fundamental principles of atmospheric dynamics and chemistry and can produce results that are independent of observed surface concentrations. The main limitations of CTMs are the computational expense of running the simulations (Fan et al., 2022) and coarse-resolution simulations may have large biases due to emissions, meteorology, and chemical processes (Wang et al., 2020b; Wang et al., 2020c).

More recently, machine learning (ML) techniques have been used to estimate surface SO_2 concentrations from satellite retrievals, meteorology, and other variables such as emission inventories and land use types. Zhang et al. (2022) used a Light Gradient Boosting Machine (LightGBM) to estimate surface SO_2 concentrations over northern China using OMI SO_2 VCDs, meteorological variables, emissions, land use classifications, population density, and others. Yang et al. (2023a) used radiances from the Geostationary Environment Monitoring Spectrometer (GEMS) satellite to estimate the surface concentrations of SO_2 and other criteria air pollutants in a multi-output random forest model. Both studies showed that ML techniques can accurately capture the spatial distribution and magnitude of the surface concentrations but had artificial biases due to nonphysical links between variables and the surface concentrations, such as interactions between certain land use types and skin temperature as shown by Zhang et al. (2022). In these studies, the ML models also incorporate spatial (e.g., longitude, latitude, population density) and/or temporal (e.g., numeric day of year, hour of day)

https://doi.org/10.5194/egusphere-2025-1735
Preprint. Discussion started: 25 April 2025

proxies to improve performance, but this can lead the model to learn the locations of cities and introduce an artificial seasonality rather than depending on measurable quantities, limiting the physical usefulness and interpretability of the model (Zhang et al., 2022; Yang et al., 2023a; Yang et al., 2023b). ML models are typically much faster to train and run than a full CTM simulation and can often utilize higher resolution data (Fan et al., 2022). Since ML models can only use statistical relationships to make predictions, they are often limited in their physical interpretability.

Although the CTM and ML methods have both been employed in estimating surface SO_2 concentrations from satellite retrievals, so far there has been a lack of direct comparisons between the two methods. Here, we estimated surface SO2 concentrations using OMI VCDs over eastern China (105-125°E, 25-45°N) from 2015-2018 to directly compare the two methods. First, we used the relationship between the surface and total column concentrations simulated by GEOS-Chem to estimate surface SO_2 concentrations from the satellite data. Then, we used a ML model to predict surface SO_2 concentrations from OMI VCDs, meteorological variables, and an emission inventory, which are all physically relevant to the spatial distribution or lifetime of SO_2. The results from each method were validated against ground-based in situ measurements from the China National Environmental Monitoring Centre (CNEMC) air quality monitoring network. Finally, we compared the performance of each method on an identical dataset for the first time to gain insights on their abilities and limitations to accurately estimate the surface SO_2 concentrations.

2 Data and methods

2.1 Study region

Eastern China has abundant anthropogenic SO_2 emissions and thus is a region with elevated surface concentrations. A map of our study region with the locations of OMI-derived SO_2 emission sources (Fioletov et al., 2022) and CNEMC monitoring sites in the study region are shown in Fig. 1. The largest sources of SO_2 in the study region come from 70 power plants, as well as five ore smelters and one area of oil and gas production (Fig. 1b). There are also approximately 1000 stations located across the region that can be used to validate the estimated surface concentrations from the satellite data (Fig. 1c). Our analysis covers the period from 2015 (the first full year of in situ measurements) to 2018 (to avoid the impacts of the COVID-19 lockdowns).

https://doi.org/10.5194/egusphere-2025-1735
Preprint. Discussion started: 25 April 2025

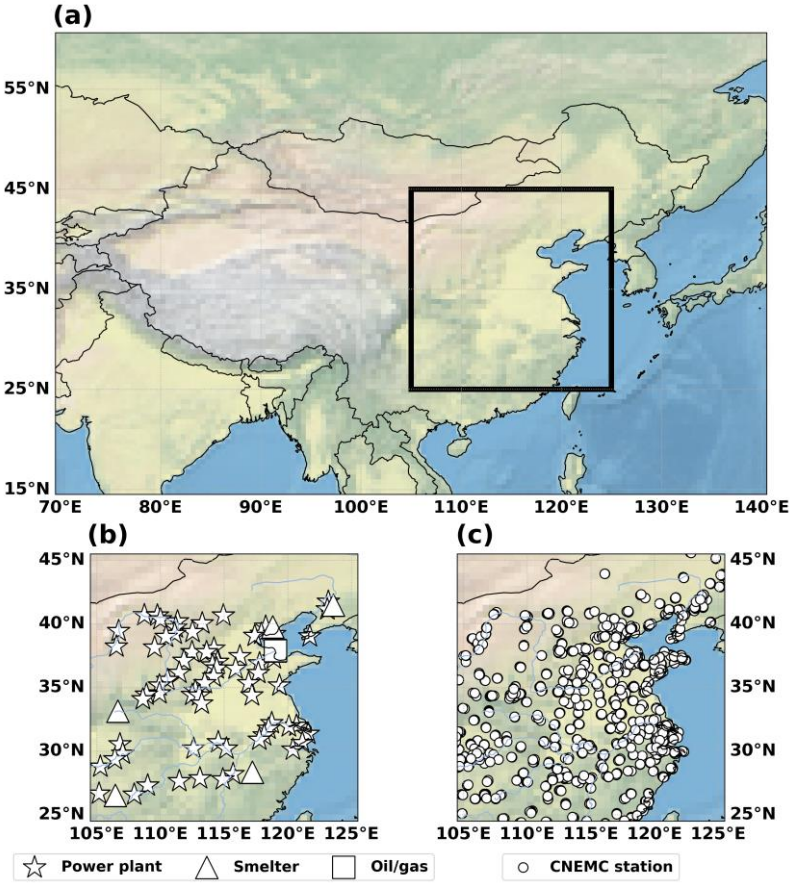

Figure 1: Maps showing the (a) study region (solid box; 105°E - 125°E, 25°N - 45°N) relative to the rest of the Asian continent, (b) locations of large SO_2 sources from the OMI emission catalogue during 2015 (Fioletov et al., 2022) including 70 power plants (stars), five ore smelters (triangles), one area of oil and gas production (square), and (c) locations of the CNEMC monitoring stations (circles).

2.2 OMI satellite data

We employed data from the Ozone Monitoring Instrument (OMI; Levelt et al., 2006), a hyperspectral ultraviolet/visible nadir solar backscatter spectrometer launched onboard the Aura satellite in 2004. Aura flies in a sun-synchronous polar orbit, and OMI is used to retrieve SO_2 VCDs with daily global coverage and a spatial resolution of 13 km x 24 km at nadir, a significant improvement from previous satellite-based instruments. The OMI overpass time of our study region ranges from approximately 12:15 pm to 2:45 pm local time. For both methods, we used the OMI Planetary Boundary Layer (PBL) SO_2 product to estimate the surface concentrations due to its main application for anthropogenic, near-surface SO_2 (Krotkov et al., 2014; Li et al., 2020b). The OMI retrievals use a principal component analysis- (PCA) based algorithm for spectral fitting based on the radiances of wavelengths between 310.5-340 nm for each row in the measurement swath (Li

https://doi.org/10.5194/egusphere-2025-1735
Preprint. Discussion started: 25 April 2025

et al., 2013; Li et al., 2020a). This version of the PCA retrievals include pixel-specific air mass factor calculations to convert slant column densities (SCDs) to VCDs rather than using a fixed value worldwide (Li et al., 2020a). The VCDs express the number of SO_2 molecules in the column and are reported in Dobson Units (DU; 1 DU = 2.69 x 10^{16} molecules cm^{-2}). To ensure good data quality, we gridded the data to 0.25° x 0.25° resolution and screened out measurements with cloud fractions greater than 0.3, solar zenith angles greater than 65°, located in the outer ten cross-track positions, or affected by the row anomaly (NASA, 2020). We also excluded extreme outliers that fell outside of five standard deviations from the mean as thresholds less than this appeared to remove legitimate data.

2.3 CNEMC ground-based monitoring data

Ground-based SO_2 concentrations from the China National Environmental Monitoring Centre (CNEMC) air quality monitoring network were used to validate the performance of each method. The concentrations were converted from μg m^{-3} to parts per billion (ppbv) following the procedure outlined in Wei et al. (2023). To ensure the ground-based measurements were temporally aligned with the OMI overpass, we averaged the hourly concentrations from 12:00 pm to 3:00 pm local time on days where there was at least one OMI observation within 40 km of the station. Like the OMI data, we also removed data that fell more than five standard deviations outside of the mean.

2.4 GEOS-Chem technique

We used simulated SVRs from the GEOS-Chem model (v14.2.2; Bey et al., 2001) to convert the OMI VCDs into surface concentrations for the CTM-based method. We conducted simulations for January, April, July, and October 2015 each with a one-month spin-up to represent the SO_2 profiles in different seasons. To reduce the computational expense, we used the monthly average SVR from each simulation to estimate the surface concentrations in the corresponding winter (DJF), spring (MAM), summer (JJA), and autumn (SON) months for all years of the study period. The model was run at a resolution of 2.5° x 2.0° with 47 vertical layers and was driven by assimilated GEOS-FP meteorology (Lucchesi, 2018) and the Community Emissions Data System (CEDS) emission inventory (Hoesly et al., 2018). The internal time steps for the chemistry and advection calculations in the model were lengthened by 50% from the default values to reduce simulation times while minimizing errors (Philip et al., 2016). We used model output at the lowest model level (~60 m above ground level) at 2:00 pm local time, the only output timestep inside the OMI overpass window. We only included GEOS-Chem data in the analysis if there was at least one valid OMI observation within the model grid cell on a given day.

The approach from Lee et al. (2011) was used to infer surface SO_2 concentrations from OMI VCDs using the GEOS-Chem (GC) simulated SO_2 profiles. The conversion was done using the following relationship:

$$S_{OMI} = \frac{\nu S_{GC}}{\nu \Omega_{GC,PBL} + \Omega_{GC,FT}} \times \Omega_{OMI}, \quad (1)$$

where S is the surface SO_2 concentration in ppbv and Ω is the SO_2 VCD in DU. The FT and PBL subscripts are the free-tropospheric and boundary layer VCDs, respectively, which were calculated relative to the GEOS-FP PBL height. Since

https://doi.org/10.5194/egusphere-2025-1735
Preprint. Discussion started: 25 April 2025

there is a significant difference in resolution between the satellite and model data, OMI VCDs were used to provide sub-model grid variability (ν) using:

$$\nu = \frac{\Omega_{OMI}}{\Omega'_{OMI}}, \quad (2)$$

where Ω_{OMI} is the OMI VCD at 0.25° resolution and Ω'_{OMI} is the average OMI VCD over the 2.5° x 2.0° GEOS-Chem grid cell. To compare the estimated concentrations to the in situ surface monitoring data, we used a 40 km averaging radius around each station to increase the amount of usable data and reduce noise in the OMI data. Since this method does not require prior knowledge of in situ measurements, the analysis in Sect. 3.1 will be performed over the full dataset.

One simplification of our approach is to use January, April, July, and October simulations for a single year (2015) to estimate the surface SO_2 concentrations over the entire study period. To evaluate this approach, we first compared the GEOS-Chem and OMI SO_2 VCDs. We found that there was no significant change in the correlation between them from 2015-2018 (Fig. S1). This indicates the spatial distributions remained similar, and the model can distinguish between relatively polluted and unpolluted areas, and thus, the SVRs in those environments. We also ran four additional GEOS-Chem simulations for January, April, July, and October 2018 to assess the year-to-year changes in the SVR. The slopes in Fig. S2 indicate that the monthly average SVR does not have a systematic change from 2015-2018 and has a maximum discrepancy of 13%. Since the spatial distribution of SO_2 and simulated SVRs remained relatively constant over time, we believe this simplification made to reduce computational expense will not have a significant impact on the results.

2.5 Machine learning technique

To estimate the surface concentrations using a ML model, we used an eXtreme Gradient Boosting regression model (XGBoost; Chen & Guestrin, 2016) to statistically relate satellite-based SO_2 VCDs, meteorological variables, and emissions data to the in situ measurements. XGBoost models use a scalable tree boosting system to efficiently train an ensemble of decision trees by adding a new tree with each training epoch and learning with each iteration (Chen & Guestrin, 2016; Friedman, 2001). We trained the model with an ensemble of 500 trees with a maximum tree depth of 15 splits, and a learning rate of 0.15 on a mean squared error loss function. Using an ensemble with more trees did not improve the performance of the model, and using a depth of 15 splits was found to be the best balance between overfitting and underfitting during training.

Our ML model was trained on a small number of variables (five) that each have known physical relationships to the spatial distribution or lifetime of SO_2. By using a small number of variables, it is easier to derive physical meaning from the ML predictions without sacrificing accuracy since the input variables are already known to affect surface SO_2 concentrations. First, we used daily OMI SO_2 VCDs to estimate the spatial distribution of SO_2. Next, we used hourly 100 m u-wind, 100 m v-wind, and PBL height (PBLH) averaged over the OMI overpass window from the European Centre for Medium-Range Weather Forecasts (ECMWF) Reanalysis v5 (ERA5; Hersbach et al., 2020; ECMWF, 2019) to account for the meteorological mixing and dispersion of SO_2. Finally, we used monthly SO_2 emissions from the CEDS inventory to

https://doi.org/10.5194/egusphere-2025-1735
Preprint. Discussion started: 25 April 2025

capture the known locations of SO_2 sources. We trained the model on logarithmic emissions since the values ranged several orders of magnitude, and logarithmic boundary layer heights to get better sensitivity to variations in low boundary layers. The model can be summarized as:

$$S_{ML} = XGBoost(\Omega_{OMI}, U_{ERA5}, V_{ERA5}, \log_{10}[PBLH_{ERA5}], \log_{10}[E_{CEDS}]), \quad (3)$$

where S_{ML} is the predicted surface concentrations from the XGBoost ML model, Ω_{OMI} is the satellite SO_2 VCD, U_{ERA5} is the u-wind, V_{ERA5} is the v-wind, $PBLH_{ERA5}$ is the boundary layer height, and E_{CEDS} is the SO_2 emissions.

We trained the model on 90% of the daily data (N = 137630) from 2015 to 2018 with meteorology and emission variables sampled to match the OMI observations. The input variables were averaged within 40 km of the CNEMC sites for training, as done in the GEOS-Chem method. The remaining 10% of the data (N = 15292) was reserved for a sample-based independent validation, as done in previous studies (e.g., Zhang et al., 2022; Yang et al., 2023a; Yang et al., 2023b). Figure 2 shows that the model had better performance with the training data (slope = 0.89; r = 0.95) compared to the testing data (slope = 0.67; r = 0.76), indicating that the model has good performance, but is slightly overfitting, a common artifact of complex machine learning models such as XGBoost.

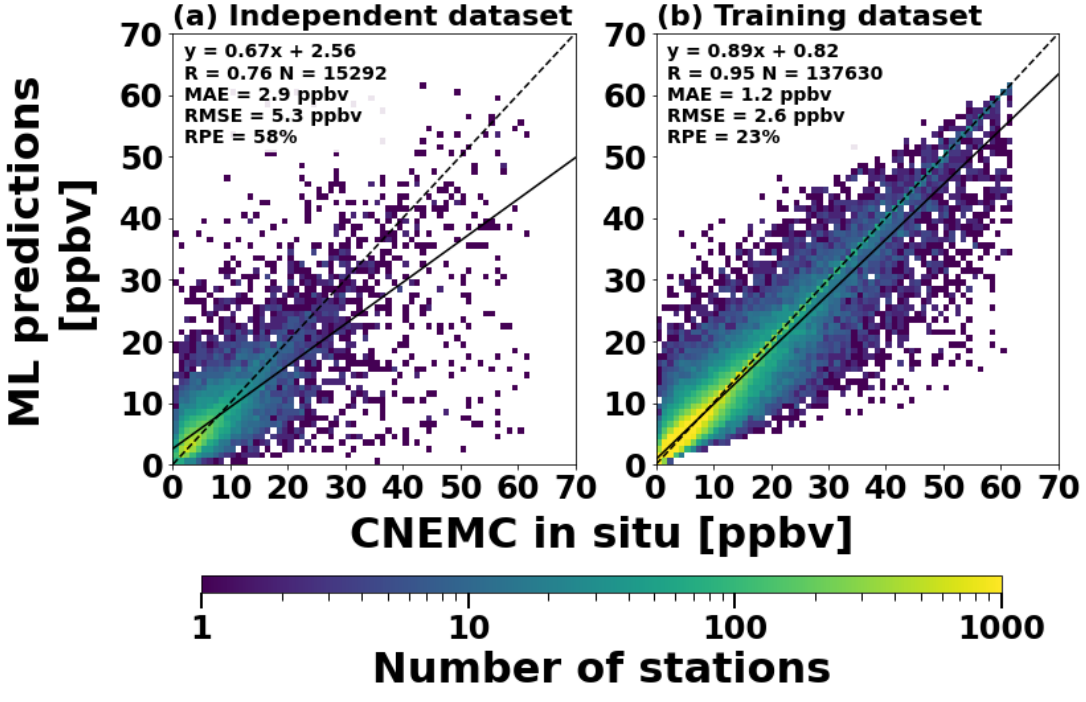

Figure 2: Scatterplots between the daily ML model predictions and CNEMC in situ measurements for the (a) independent dataset and (b) training dataset. Each panel includes a linear regression analysis with best fit line (solid line) and discrepancy statistics for the estimated surface SO_2 concentrations compared to in-situ measurements. The scatterplots are binned every 1 ppbv. The dashed line indicates the 1:1 line.

https://doi.org/10.5194/egusphere-2025-1735
Preprint. Discussion started: 25 April 2025

2.6 Evaluation metrics

To quantify the discrepancies between the in situ surface SO_2 concentrations and the estimates using the GEOS-Chem and ML methods, we used several different metrics that were utilized in previous studies (e.g., Yang et al., 2023b; Zhang et al., 2021; Zhang et al., 2022) including the mean absolute error (MAE; Eq. 4), root mean squared error (RMSE; Eq. 5), and relative percent error (RPE; Eq. 6),

$$MAE = \frac{1}{N}\sum_i^N \left|S_{est,i} - S_{CNEMC,i}\right|, \quad (4)$$

$$RMSE = \sqrt{\frac{1}{N}\sum_i^N \left(S_{est,i} - S_{CNEMC,i}\right)^2}, \quad (5)$$

$$RPE = \frac{1}{N}\left(\sum_i^N \left|\frac{S_{est,i} - S_{CNEMC,i}}{S_{CNEMC,i}}\right|\right) \times 100\%, \quad (6)$$

where N is the number of stations, S_{est} is the estimated surface concentration from the GEOS-Chem or ML method, and S_{CNEMC} is the in situ surface concentration. Previous studies have also used slopes and correlations from linear regression analyses between the estimated and in situ concentrations to assess the magnitude and spatial distribution, respectively (e.g., Kharol et al., 2017; Lee et al., 2011; McLinden et al., 2014). The GEOS-Chem and ML results were compared to previous studies, as well as to each other. The comparison between the two methods in our study were made using an identical, independent (i.e., retained from ML training) dataset.

3 Estimations of surface SO_2 Concentrations from OMI satellite data

3.1 Evaluation of the GEOS-Chem method

Maps, histograms, and scatterplots of the annual mean surface SO_2 concentrations from the GEOS-Chem method and CNEMC in situ measurements are shown in Fig. 3. Both datasets have a similar spatial distribution with the highest concentrations in the North China Plain (Fig. 3), a highly industrialized region with many anthropogenic sources of SO_2 (Fig. 1b). The average correlation between the estimated and in situ concentrations is 0.58, indicating that the GEOS-Chem method can distinguish between polluted and clean areas (Fig. 3). The GEOS-Chem method also captures a 45% decrease in the concentrations from 2015-2018, matching the change from the monitoring network (Fig. 3). The decrease in SO_2 is due to the regulation of emissions, which has been previously reported in previous studies using satellite VCDs (Li et al., 2017; Wang et al., 2020a) and surface concentrations (Wei et al., 2023; Zhang et al., 2021). Despite the similarities in the spatial distribution and temporal trends, the surface concentrations obtained from the GEOS-Chem method are significantly underestimated. The slope between the estimated and in situ concentrations is 0.24 with an RPE around 75% (Fig. 3). The discrepancy in the estimated concentrations is also apparent in the frequency distributions with a peak and mean value at lower concentrations and a smaller range compared to the in situ measurements. The concentrations from the GEOS-Chem method and CNEMC measurements were also separated by season and averaged from 2015-2018. As shown in Fig. S3, the

https://doi.org/10.5194/egusphere-2025-1735
Preprint. Discussion started: 25 April 2025

GEOS-Chem method was able to accurately capture the spatial distribution and seasonality of the in situ measurements but still suffered from underestimation.

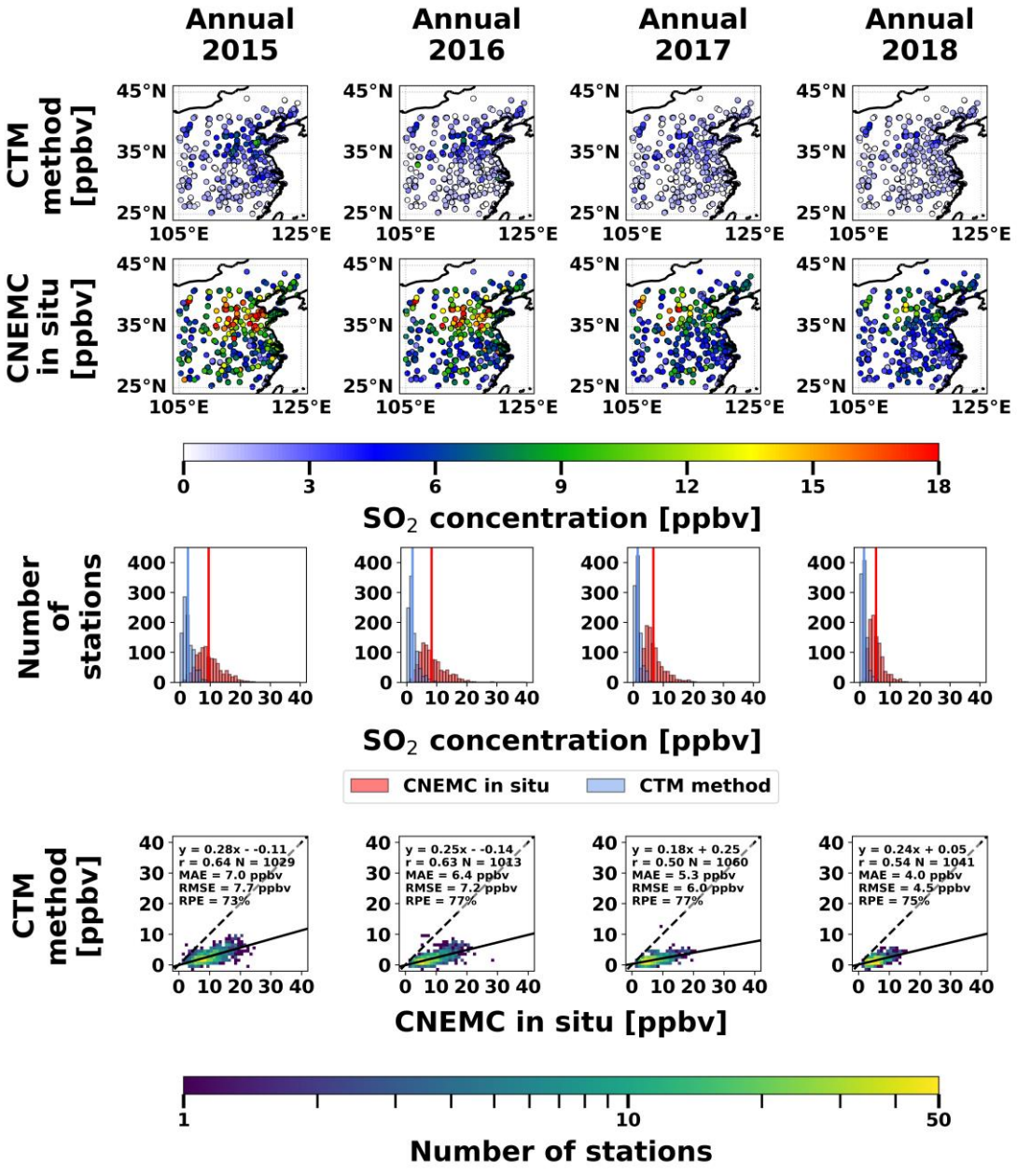

Figure 3: Spatial distributions of the annual average surface SO_2 concentrations from the CTM-based method (top row) and CNEMC in situ measurements (second row), histograms of the surface concentrations from each dataset with vertical bars representing the means (third row), and scatterplots between the two datasets (bottom row). Each column represents a different year in the study period. Histograms and scatterplots are binned every 1 ppbv. Each scatterplot is colored by the number of

https://doi.org/10.5194/egusphere-2025-1735
Preprint. Discussion started: 25 April 2025

stations in each bin and includes a linear regression analysis with the best fit line (solid lines), 1:1 line (black dashed line), MAE, RMSE, and RPE.

Table 1 summarizes the results from our study compared to previous studies using the CTM-based method. These previous studies were primarily focused on estimating annual mean surface SO_2 concentrations using OMI VCDs and CTMs of varying resolution. The studies by Lee et al. (2011) and McLinden et al. (2014) each utilized the OMI band residual difference (BRD) SO_2 product and used SVRs from coarse-resolution and high-resolution CTMs, respectively. McLinden et al. (2014) outperformed Lee et al. (2011) with slopes of 0.88 and 0.79, respectively, and correlations of 0.91 and 0.81, respectively. Similarly, our study and Kharol et al. (2017) both use the OMI PCA SO_2 product and used SVRs from coarse-resolution and high-resolution CTMs, respectively. Our study had slightly worse performance than Kharol et al. (2017) with slopes of 0.24 and 0.39, respectively, and correlations of 0.58 and 0.61, respectively. These two sets of studies suggest that given the same OMI data, the model resolution plays an important role in accurately estimating the surface concentrations compared to the in situ observations, assuming that the surface monitoring data are accurate. Previous studies have also shown that there are differences in SO_2 as a result of different retrieval algorithms and sensors (Wang et al., 2020a). The higher slopes from the BRD product may be due to a high bias in the retrievals in polluted areas whereas the PCA product is thought to be more accurate (Li et al., 2013). Additionally, the slope of 0.75 from Kharol et al. (2017) and the results from Zhang et al. (2021) are based on applying a scaling factor to the in situ measurements to eliminate some of the bias, so these results are not directly comparable to our study.

https://doi.org/10.5194/egusphere-2025-1735
Preprint. Discussion started: 25 April 2025

Table 1: Comparison of study design (satellite data, model name and resolution, study location and study period) and performance metrics (mean absolute error, root mean square error, relative percent error, slope, and correlation) between our study and previous studies that utilized the CTM-based method. NR indicates that the value was not reported, and asterisks (*) indicate a scaling factor applied to the in situ surface concentrations.

Study	Satellite data	CTM (resolution)	Study location (time period)	MAE [ppbv]	RMSE [ppbv]	RPE [%]	Slope [-]	Correlation [-]
Our study	OMI SO_2 PCA	GEOS-Chem, (2.5° x 2.0°)	Eastern China (2015-2018)	5.7	6.3	74	0.23	0.58
Lee et al. (2011)	OMI SO_2 BRD	GEOS-Chem, (2.5° x 2.0°)	North America (2006)	NR	NR	NR	0.79	0.81
McLinden et al. (2014)	OMI SO_2 BRD	GEM-MACH, (15 km)	Canadian oil sands (2005-2011)	NR	NR	NR	0.88	0.91
Kharol et al. (2017)	OMI SO_2 PCA	GEM-MACH, (15 km)	North America (2005-2015)	NR	NR	NR	0.39/0.75*	0.61
Zhang et al. (2021)	OMI SO_2 PCA	MOZART, 1.9° x 2.5° Resolution	China (2014)	NR	3.9	19	0.83*	0.86

Inaccuracies in the CTM-based method can be partially attributed to noise in the satellite data. Individual VCD retrievals have very large uncertainties (60-130%; Li et al., 2020a), making it difficult to compare to the ground-based measurements on short timescales. However, the noise in the data can decrease with temporal averaging by a factor of $n^{1/2}$

https://doi.org/10.5194/egusphere-2025-1735
Preprint. Discussion started: 25 April 2025

where n is the number of measurements being averaged (Krotkov et al., 2008). As a result, longer averaging periods (i.e., annual means) tend to have better performance than shorter timescales (i.e., seasonal means). The CTM resolution is also important for obtaining accurate surface concentrations. Coarse grid cells may smooth out SO_2 hotspots potentially resulting in an SVR that is too small. This may account for the consistent underestimation observed from this method and the relatively better performance in Kharol et al. (2017) with a higher resolution CTM.

3.2 Evaluation of the machine learning method

The spatial distribution, frequency distribution, and validation scatterplots of the ML and CNEMC annual mean surface SO_2 concentrations from the independent testing dataset are shown in Fig. 4. The ML model estimated the surface concentrations more accurately than the GEOS-Chem method. The average spatial correlation was 0.77, and the ML predictions also matched the 45% decline from 2015 to 2018 observed from the CNEMC network. The most significant improvement compared to the GEOS-Chem method is the RPE of the ML method is much smaller at 33%, and the average slope is 0.69, indicating both less discrepancy and underestimation, respectively. The shapes of the ML-based frequency distributions agree well with the CNEMC observations with peaks at the same concentrations and similar ranges (Fig. 4). The ML-derived and in situ concentrations were also assessed using the seasonal concentrations averaged from 2015-2018. As shown in Fig. S4, the ML method was able to capture the spatial distribution, seasonality, and magnitudes of the surface concentrations on the seasonal data more accurately than the GEOS-Chem method.

https://doi.org/10.5194/egusphere-2025-1735
Preprint. Discussion started: 25 April 2025

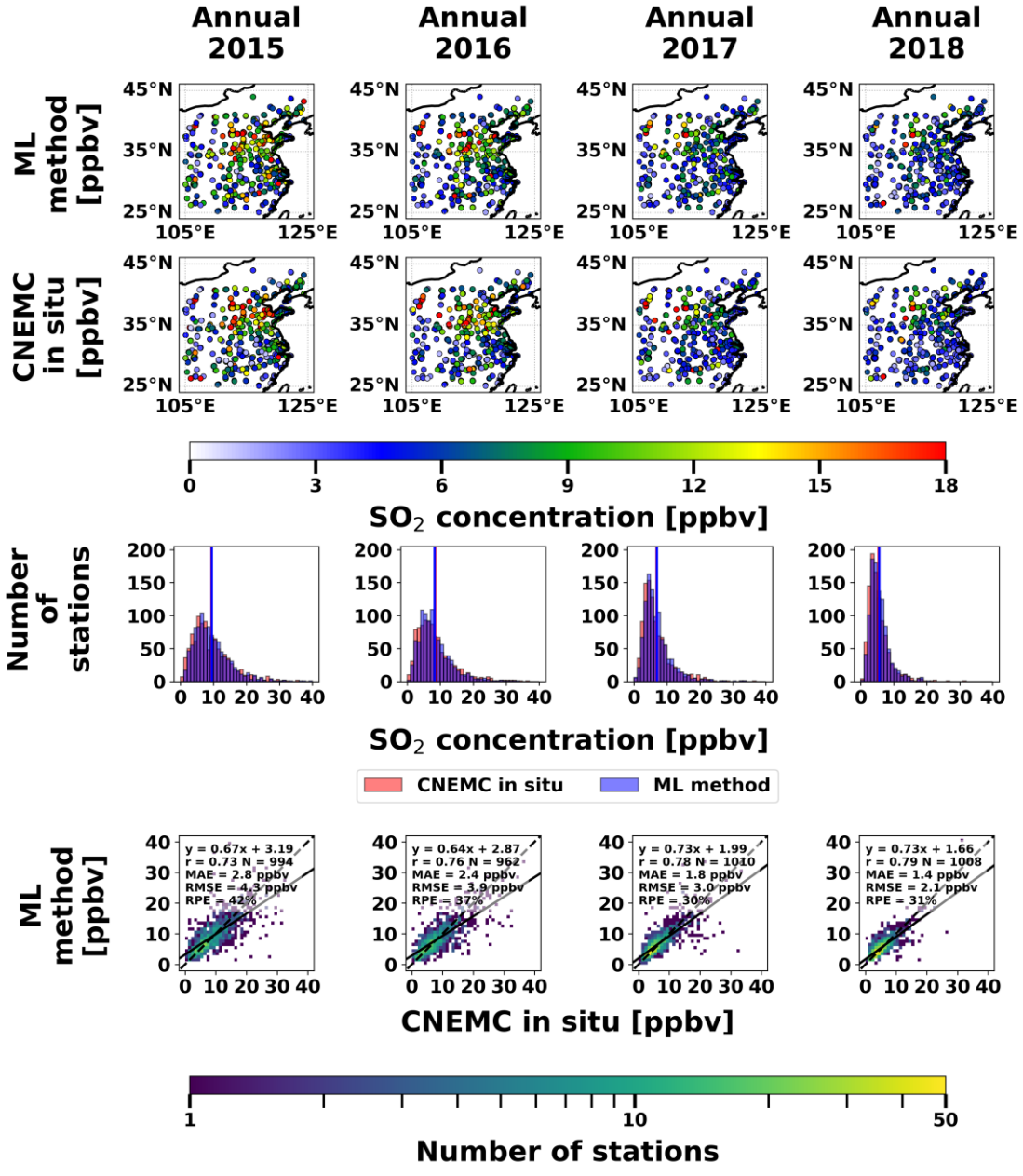

Figure 4: Spatial distributions of the annual average surface SO_2 concentrations from the ML-based method (top row) and CNEMC in situ measurements (second row), histograms of the surface concentrations from each dataset with vertical bars representing the means (third row), and scatterplots between the two datasets (bottom row). Each column represents a different year in the study period. Histograms and scatterplots are binned every 1 ppbv. Each scatterplot is colored by the number of stations in each bin and includes a linear regression analysis with the best fit line (solid lines), 1:1 line (black dashed line), MAE, RMSE, and RPE.

https://doi.org/10.5194/egusphere-2025-1735
Preprint. Discussion started: 25 April 2025

Previous studies have shown that ML models can skillfully capture day-to-day variations in surface SO_2 concentrations in addition to the annual and seasonal means as summarized in Table 2 (e.g., Zhang et al., 2022; Yang et al., 2023b). The estimated daily surface concentrations from our independent testing dataset had a slope of 0.67, correlation of 0.76, and RPE of 58% compared to the in situ measurements, indicating accuracy on short timescales (Fig. 2; Table 2). The performance of our model was comparable to previous studies but had a slightly larger discrepancy (Table 2). Our ML model only used five predictors compared to nine in Yang et al. (2023b) and 66 in Zhang et al. (2022), which may partially account for the increased discrepancy. Additionally, our study did not use any spatial or temporal proxies, which could also explain the slight reduction in performance compared to other studies that have used them.

https://doi.org/10.5194/egusphere-2025-1735
Preprint. Discussion started: 25 April 2025

Table 2: Comparison of study design (satellite data, machine learning model type and number of predictors, study location and study period) and performance metrics (mean absolute error, root mean square error, relative percent error, slope, and correlation) between our study and previous studies that utilized a ML-based method. NR indicates that the value was not reported.

Study	Satellite data	Machine learning model (number of predictors)	Study location (time period)	MAE [ppbv]	RMSE [ppbv]	RPE [%]	Slope [-]	Correlation [-]
Our study	OMI SO_2 PCA	XGBoost (5)	Eastern China (2015-2018)	3.0	5.2	59	0.67	0.75
Zhang et al. (2022)	OMI SO_2 PCA	LightGBM (66)	Northern China (2013-2019)	NR	4.0	39	NR	0.94
Yang et al. (2023b)	Landsat-8 visible and infrared reflectance	Deep neural network multi-task learning (9)	China (2019)	3.5	5.7	47	0.76	0.85

We performed a permutation importance analysis to assess how each predictor impacted the model predictions. Figure 5a indicates that the PBLH and OMI SO_2 VCDs are the two most influential predictors followed by emissions and wind speeds. Scatterplots between each ML predictor variable and the ML estimated surface SO_2 concentrations with Spearman rank coefficients (r_s) are shown in Figs. 5b-f. The ML-derived SO_2 concentrations increase with larger SO_2 VCDs and emissions, as well as decrease with increasing PBLH and wind speeds (Figs. 5b-f). These trends are consistent with the expected physical relationships between each variable and surface SO_2 concentrations in the real atmosphere. Large OMI VCDs and emissions indicating areas of high SO_2 loading, and elevated PBLHs and wind speeds lead to mixing and the

https://doi.org/10.5194/egusphere-2025-1735
Preprint. Discussion started: 25 April 2025

dilution of SO_2. The r_s values are small, indicating that the model may be making predictions based on the interactions between variables rather than any individual predictor. The small number of predictors used in our model allows us to link the ML predictions to known atmospheric processes, adding confidence to the model in its ability to accurately estimate the surface concentrations.

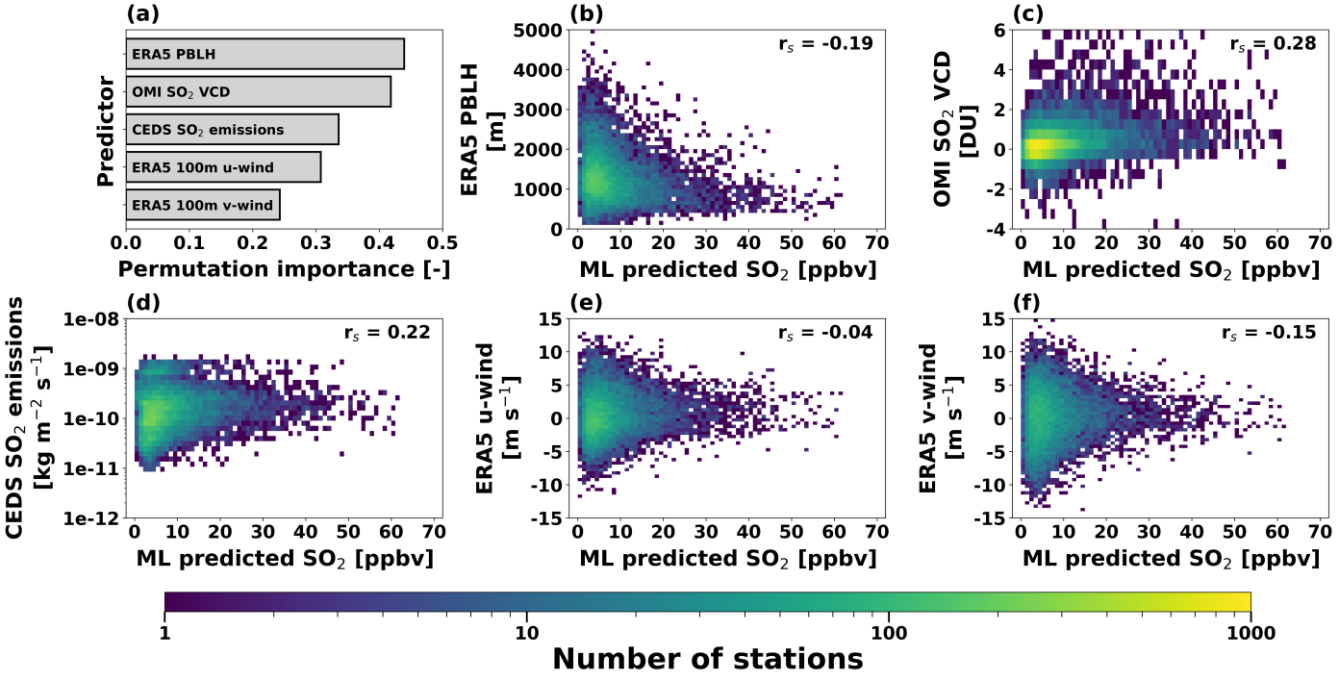

Figure 5: Evaluation of the daily ML-predicted surface concentrations using (a) permutation importance analysis, and scatterplots showing the ML predictor variables against the ML estimated surface SO_2 concentrations for (b) ERA5 PBLH, (c) OMI SO_2 VCDs, (d) CEDS SO_2 emissions, (e) ERA5 U-Winds, and (f) ERA5 V-Winds. Each scatterplot is colored by the number of stations in each bin and includes the Spearman rank coefficient (r_s).

4 Comparing results from the GEOS-Chem and machine learning methods

The results from the GEOS-Chem method in Sect. 3.1 were based on the full dataset since the methodology produces results that are independent of the in situ monitoring data. However, the results from the ML method in Sect. 3.2 were only based on 10% of the data that was not used for training and reserved for an independent validation. The comparison of these results is still important but does not provide a direct comparison of their performance. Here, the GEOS-Chem and ML methods will be compared using the independent testing dataset (i.e., retained from ML training) to assess the relative performance of each method given identical data. First, each technique will be validated at the CNEMC measurement sites in Sect. 4.1, similar to the analyses in Sect. 3. Then, both methods will be used to create gridded surface

https://doi.org/10.5194/egusphere-2025-1735
Preprint. Discussion started: 25 April 2025

SO_2 concentrations in Sect. 4.2 to assess how effective both methods are for filling in the gaps of the CNEMC monitoring network, one of the main motivations for estimating surface concentrations from satellite data.

4.1 Performance on independent data

Scatterplots between the in situ concentrations and estimates of the surface concentrations from both the GEOS-Chem and ML methods for the identical testing dataset are shown in Fig. 6. The surface concentrations estimated by the ML model are much closer to the in situ measurements (1:1 line) than the GEOS-Chem method, which is consistent with the previous results in Figs. 3-4. For the annual mean concentrations, the ML method had an average slope of 0.69 and correlation of 0.77, compared to values of 0.18 and 0.30 from the GEOS-Chem method, respectively (Figs. 6a-d). The ML model also outperforms the GEOS-Chem method on the seasonal data averaged over 2015-2018. The average slope and correlation of 0.64 and 0.73, compared to 0.19 and 0.31, respectively (Figs. 6e-h). The GEOS-Chem method performed worse on this smaller dataset compared to the full dataset in Sect. 3.1 due to less temporal averaging, leading to larger discrepancies with the in situ measurements. As shown in Fig. S5, there is a smaller decrease in the performance of the ML method compared to the GEOS-Chem method when assessing the performance for individual seasons. The slope and correlation for the ML method decreased to 0.59 and 0.67, compared to 0.15 and 0.22 for the GEOS-Chem method, respectively (Fig. S5). Despite the smaller amounts of data in the independent dataset and for individual seasons, the ML method still accurately captures the spatial distribution and magnitudes of the surface SO_2 concentrations, indicating better consistency with the CNEMC measurements than the GEOS-Chem method.

https://doi.org/10.5194/egusphere-2025-1735
Preprint. Discussion started: 25 April 2025

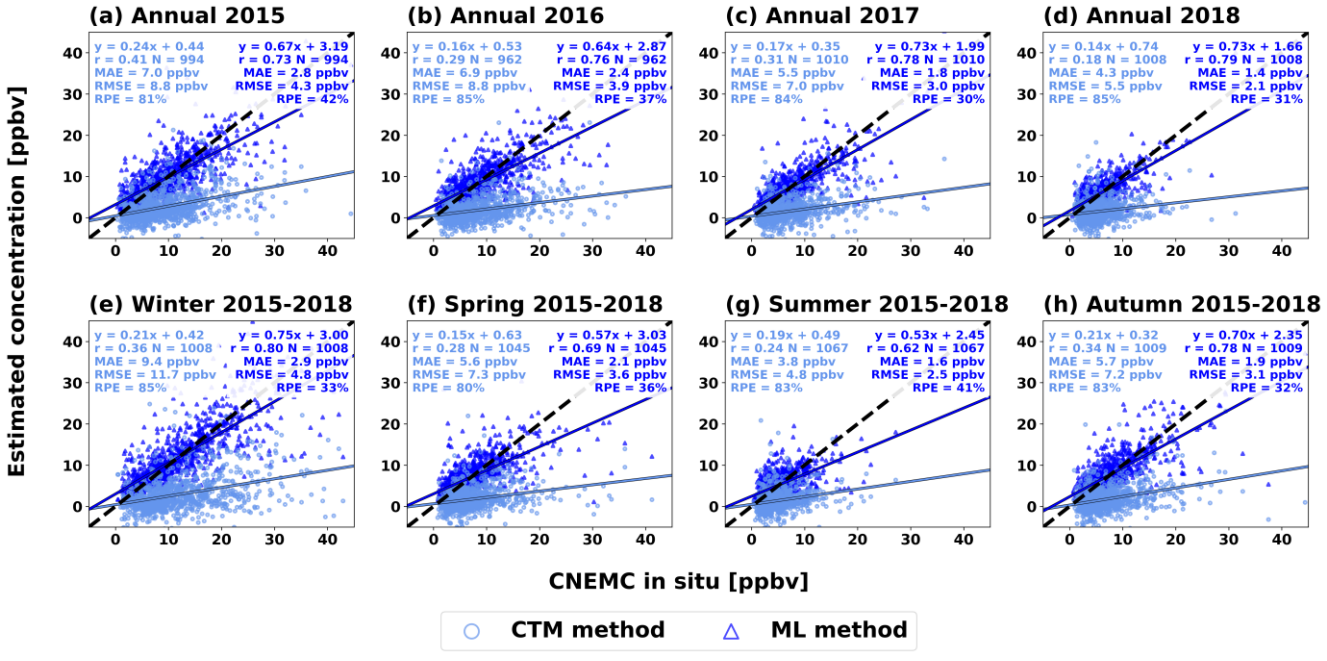

Figure 6: Scatterplots showing the estimated surface SO_2 concentrations from the GEOS-Chem method (light blue squares) and ML method (dark blue triangles) against the in situ measurements from the independent dataset for (a-d) annual mean concentrations for each year in the study period, and (e-h) the 2015-2018 mean concentrations separated by season. Each scatterplot includes a linear regression analysis with the best fit line (solid lines), 1:1 line (black dashed line), MAE, RMSE, and RPE.

Time series of the annual and seasonal mean surface SO_2 concentrations from the in situ measurements, and estimated concentrations from the GEOS-Chem and ML methods are shown in Figs. 7a-b. The ML estimated concentrations were much more accurate than the GEOS-Chem method compared to the CNEMC in situ concentrations. The overall mean ML concentrations had an average discrepancy of 5% with the in situ measurements, compared to a 58% discrepancy from the GEOS-Chem method (Figs. 7a-b). The ML method also captured the same temporal variations as the in situ measurements with a 44% decrease in concentrations from 2015-2018, and an average seasonal fluctuation by a factor of 1.9 (Figs. 7a-b). The GEOS-Chem method also had good agreement in the temporal trends of the in situ measurements with a 36% decrease from 2015-2018 and a seasonal fluctuation by a factor of 2.4 between the winter and summer, but not as good as the ML method (Figs. 7a-b). Despite the similarities in the overall and seasonal variations, the greatest difference between the time series of the two methods was the magnitude of the concentrations, as shown in Sect. 3.

https://doi.org/10.5194/egusphere-2025-1735
Preprint. Discussion started: 25 April 2025

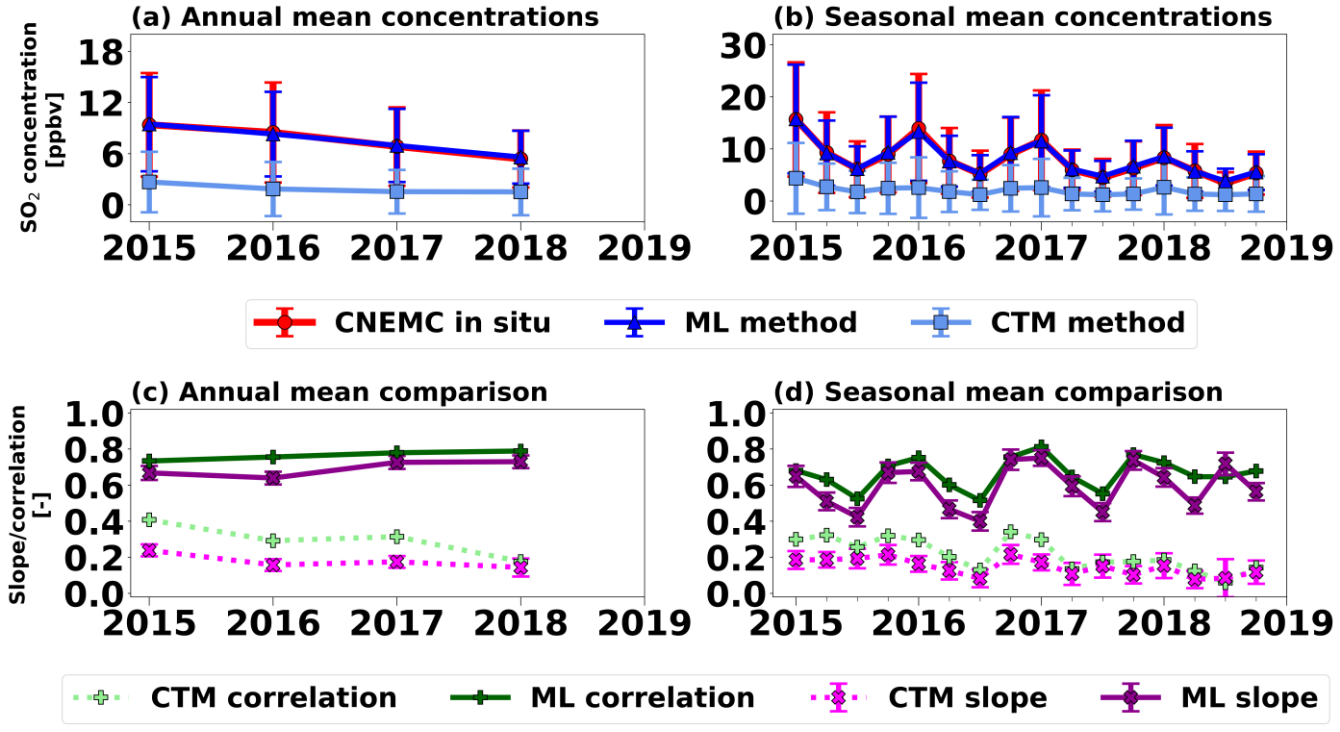

Figure 7: Time series of the surface SO_2 concentrations from the GEOS-Chem (CTM) method (light blue squares), ML method (dark blue triangles), and CNEMC in situ measurements (red circles) from the independent dataset as (a) annual and (b) seasonal means, as well as the slopes (pink x's) and correlations (green plus signs) from the (c) annual and (d) seasonal mean validations between the GEOS-Chem (CTM) method (dashed line) and ML method (solid line) with the in situ measurements. Error bars on the concentrations represent a 1 standard deviation uncertainty, and error bars on the slopes represent a 95% confidence interval based on the standard error of the linear regression fit.

To assess how the accuracy of each method changes over time, time series of the slopes and correlations from the individual annual and seasonal comparisons between the estimated and in situ surface concentrations (from Fig. S5) are shown in Figs. 7c-d. For the entire study period, the performance of the ML method was much more accurate than the GEOS-Chem method as indicated by the higher slopes and correlations (Figs. 7c-d). Additionally, the GEOS-Chem method suffered from a decrease in accuracy over time alongside declining SO_2 concentrations while the ML method remained stable (Figs. 7c-d). The accuracy of the CTM-based method is highly dependent on noise in the satellite data. Smaller datasets with less temporal averaging tend to have more noise, which leads to worse performance. Additionally, as SO_2 loading decreases, it becomes harder to detect from the satellite, introducing additional noise over time. Comparatively, the ML method is more resistant to noise in the satellite data. As the SO_2 VCDs decreased, the ML predictions became more reliant upon meteorological predictors to estimate the surface concentrations, limiting the impact of the noisy satellite data (Figs. S6a-d). The accuracy of the ML method has a distinct seasonality with generally better performance in the winter and worse in the summer (Fig. 7d). The PBLH and OMI SO_2 VCDs are dominant predictors in the winter compared to CEDS

https://doi.org/10.5194/egusphere-2025-1735
Preprint. Discussion started: 25 April 2025

emissions and PBLH in the summer (Figs. S6e-h). The CEDS emissions are less consistent with the in situ measurements than the OMI VCDs with correlations of 0.15 and 0.29, respectively, which may account for the increased discrepancy of the ML-derived concentrations during the summer.

In summary, both methods captured the same temporal variations as the in situ measurements, but the ML method performed better and had more stable performance over time than the CTM-based method, which had decreasing performance due to more noise in the satellite data from decreasing SO_2 loading.

4.2 Comparison of gridded products

Here, the GEOS-Chem and ML methods will be used to create high-resolution gridded products of surface SO_2 concentrations to assess how effective each technique is for filling in the gaps of the CNEMC air quality monitoring network. The gridded annual mean surface SO_2 concentrations from the ML and GEOS-Chem methods are shown in Fig. 8 at 0.25° horizontal resolution. Both methods have similar spatial distributions to one another over land with the highest concentrations in the North China Plain and lower concentrations elsewhere. Over land, each method also has a spatial distribution similar to the retrieved SO_2 VCDs from OMI as shown in Fig. S7a-d. Over the oceans, there is disagreement in the spatial distributions with the ML method producing high concentrations and the CTM method producing low concentrations. Since the ML predictions are significantly affected by boundary layer heights (Fig. 5), the model is most likely incorrectly associating the low marine boundary layer with areas elevated pollutants typical of low continental boundary layers, as shown in Fig. 8. Inaccuracies over the oceans have also been reported in Kang et al. (2021) where ML was used to estimate surface concentrations of NO_2 and ozone and were attributed to a lack of training data for the ML model in these locations. Since the ML model was only trained for conditions over land, it is not able to make accurate predictions over the ocean or other areas that are different from where the model was trained. As a result, the CTM-based method may be more reliable for estimating the surface SO_2 concentrations in locations with a lack of surface observations where a ML model cannot be trained.

As shown in Fig. 8, both gridded products captured the decrease in annual mean concentrations from 2015 to 2018 observed at the CNEMC sites. Both methods were also able to capture the seasonal variations in their gridded products with the highest concentrations in the winter and lowest concentrations in the summer, as shown in Fig. S8. The seasonal surface SO_2 concentrations were also still consistent with the OMI SO_2 VCDs (Fig. S7e-h). Although it is not possible to validate the gridded products, since the ML method had more accurate spatial distributions, temporal variations, and magnitudes than the CTM method at the CNEMC sites, the gridded product is likely to be more accurate as well, but only over land. The unexpected area of elevated concentrations over the oceans exposed a major limitation of the ML method and suggests that future work in improving the CTM-based method may be worthwhile, especially for estimating surface SO_2 concentrations in locations where training data are not available.

https://doi.org/10.5194/egusphere-2025-1735
Preprint. Discussion started: 25 April 2025

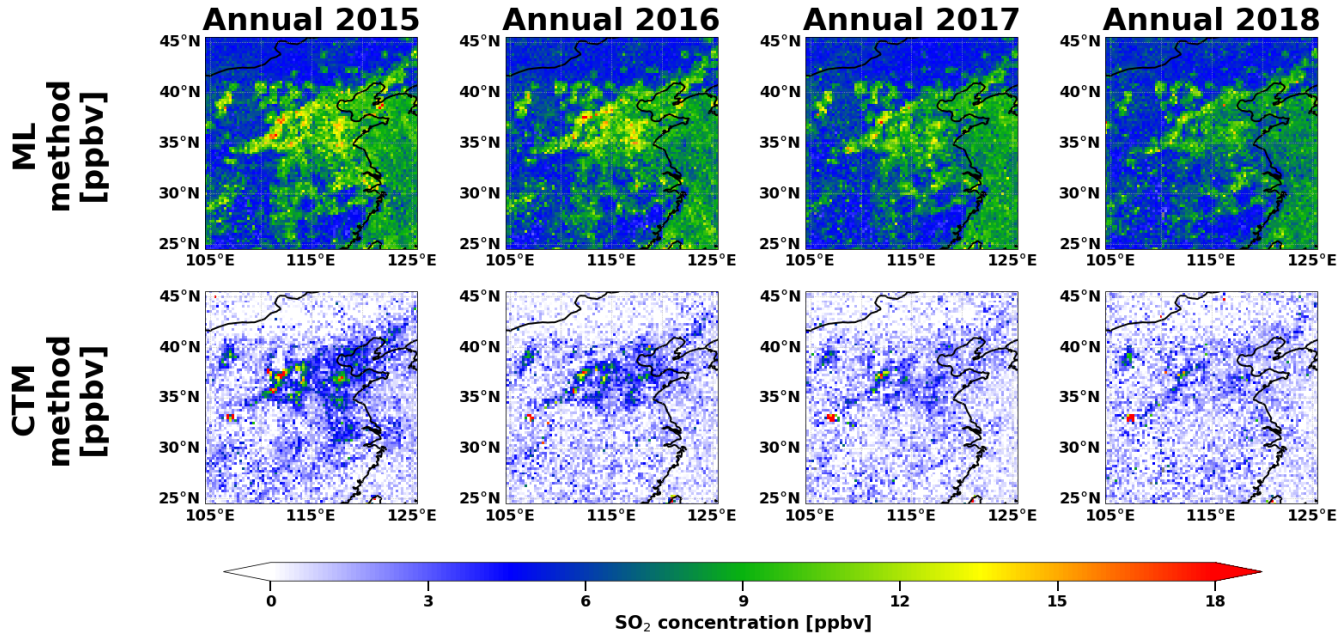

Figure 8: Maps of the annual mean surface SO_2 concentrations in ppbv from the ML method (top row) and GEOS-Chem method (bottom row) over the study area at 0.25° horizontal resolution. Each column represents a different year of the study period (from left to right: 2015, 2016, 2017, and 2018).

5 Conclusion and discussion

We estimated surface SO_2 concentrations over eastern China from 2015-2018 using OMI satellite data with two different methods: the GEOS-Chem model to convert the OMI SO_2 VCDs into surface concentrations, and an XGBoost model to statistically relate OMI SO_2 retrievals, ERA5 meteorology, and CEDS SO_2 emissions to in situ surface concentrations. We found that the ML method had better performance than the GEOS-Chem method at estimating the surface concentrations when validated against in situ measurements from the CNEMC air quality monitoring network. The ML method had a discrepancy of ~30% with no significant bias (slope = 0.69), whereas the GEOS-Chem method had a discrepancy of ~75% with a significant underestimation (slope = 0.24). To our knowledge, this is the first study to directly compare the relative performance of the CTM- and ML-based methods for estimating surface SO_2 concentrations from satellite data.

Despite the underestimation, the GEOS-Chem method produced surface SO_2 concentrations that had similar spatial distributions (r = 0.58) and temporal patterns as the CNEMC in situ measurements, similar to previous studies using the CTM-based method. To obtain a good estimate of the spatial distribution, the CTM method requires averaging data over seasonal or annual timescales to reduce the noise in the satellite retrievals, and the underestimation of this method is likely due to the coarse resolution of GEOS-Chem smoothing out the SVR near SO_2 hotspots. The CTM-based method also suffered from decreasing accuracy over time due to decreasing SO_2 loading. In addition to lower discrepancies, the ML

https://doi.org/10.5194/egusphere-2025-1735
Preprint. Discussion started: 25 April 2025

method outperformed the CTM method in terms of the spatial distribution (r = 0.77) and temporal variations. The success of the ML method was especially apparent for smaller datasets that have limited temporal averaging and thus higher noise in the OMI data, which was also indicated by the accuracy over time. Even though our ML model was only based on five input variables, the results were similar to previous studies that used far more predictors. The small number of predictors also allowed us to relate the model predictions and input variables to known physical processes such as pollutant emissions and dispersion, thus lending more confidence in our ML model as compared with other "black box" ML models. Finally, both methods were used to create high-resolution gridded products to provide estimates of surface SO_2 concentrations in locations that do not have access to ground-based air quality monitoring measurements. This analysis exposed a major limitation in the ML method where it produced unrealistic spatial distributions of SO_2 over the ocean since it was only trained on data from over the land. Despite the underestimation of the CTM method, there is still value in using it to estimate surface SO_2 concentrations in locations where there is no training data available for developing ML-based techniques, but future steps should be taken to decrease the underestimation of this method.

In the future, these methods should be applied to higher-resolution satellite data, which may help to improve the results. OMI can only detect sources as small as 30 kt yr^{-1}, but newer instruments like the Tropospheric Monitoring Instrument (TROPOMI; Veefkind et al., 2012) or can detect sources as small as 8 kt yr^{-1} (Fioletov et al., 2023). Newer polar orbiting satellites like TROPOMI and geostationary satellites like Tropospheric Emissions: Monitoring of Pollution (TEMPO; Zoogman et al., 2017) may offer future opportunities to estimate surface concentrations of air pollutants at even higher resolution. This also may improve the accuracy of both methods, especially if higher-resolution CTMs are also utilized. Additionally, this study only focused on SO_2, but both methods can also be applied to other air pollutants such as NO_2, ozone, and particulate matter to see if the relative performance of each method is similar for other species. Since these two methods can utilize space-based measurements to fill in the gaps of ground-based air quality networks, investigating their relative performance as improvements are made to the satellite data, CTMs, and ML models is critical for monitoring near-surface air pollution with high accuracy in locations where traditional observations are not possible.

Code and data availability

All data used in this work are open source. The OMI PBL SO_2 VCDs are available at https://doi.org/10.5067/Aura/OMI/DATA2023, and the OMI emission catalogue is available at https://so2.gsfc.nasa.gov/measures.html. The GEOS-Chem source code is available at https://github.com/geoschem/GCClassic, and the GEOS-Chem input data, including the CEDS emission inventory, is available at https://geos-chem.s3.amazonaws.com/index.html. The ERA5 meteorology data are available at https://nsf-ncar-era5.s3.amazonaws.com/index.html. The CNEMC in situ measurements were obtained from http://www.cnemc.cn. The XGBoost model was developed using the scikit-learn (https://scikit-learn.org/stable/) and XGBoost

https://doi.org/10.5194/egusphere-2025-1735
Preprint. Discussion started: 25 April 2025

(https://xgboost.readthedocs.io/en/stable/) Python packages. Finally, all maps were made with Natural Earth via the Cartopy Python package (https://scitools.org.uk/cartopy).

Supplement link

To be added.

Author contributions

ZW conducted the data analysis, prepared the paper, and created figures. ZW, CL, FL, and SL contributed to the development of the GEOS-Chem analysis in the paper. ZW, CL, SWF, and SL contributed to the development of the machine learning analysis in the paper. HZ and JW provided the CNEMC in situ data. All authors provided feedback and improvements to the paper.

Competing interests

The authors declare that they have no conflicts of interest.

Financial support

We acknowledge funding support from the National Science Foundation (Award numbers 2209772 and 2107916).

References

Bey, I., Jacob, D. J., Yantosca, R. M., Logan, J. A., Field, B. D., Fiore, A. M., Li, Q., Liu, H. Y., Mickley, L. J., and Schultz, M. G.: Global modeling of tropospheric chemistry with assimilated meteorology: Model description and evaluation, J. Geophys. Res. Atmos., 106, 23073–23095, doi:10.1029/2001JD000807, 2001.

Chen, T., and Guestrin, C.: XGBoost: A Scalable Tree Boosting System, Proc. 22nd ACM SIGKDD Int. Conf. Knowl. Discov. Data Min., 785–794, doi:10.1145/2939672.2939785, 2016.

China National Environmental Monitoring Centre (CNEMC): http://www.cnemc.cn, last access: 28 April 2024.

Engdahl, R. B.: A Critical Review of Regulations for the Control of Sulfur Oxide Emissions, J. Air Pollut. Control Assoc., 23, 364–375, doi:10.1080/00022470.1973.10469782, 1973.

European Centre for Medium-Range Weather Forecasts (ECMWF): ERA5 Reanalysis (0.25 Degree Latitude-Longitude Grid) (Updated monthly), Res. Data Arch. Natl. Cent. Atmos. Res., Comput. Inf. Syst. Lab., doi:10.5065/BH6N-5N20, 2019, last access: 2 Mar 2025.

https://doi.org/10.5194/egusphere-2025-1735
Preprint. Discussion started: 25 April 2025

Fan, K., Dhammapala, R., Harrington, K., Lamastro, R., Lamb, B., and Lee, Y.: Development of a Machine Learning Approach for Local-Scale Ozone Forecasting: Application to Kennewick, WA, Front. Big Data, 5, 781309, doi:10.3389/fdata.2022.781309, 2022.

Fioletov, V., McLinden, C. A., Griffin, D., Abboud, I., Krotkov, N., Leonard, P. J. T., Li, C., Joiner, J., Theys, N., and Carn, S.: Multi-Satellite Air Quality Sulfur Dioxide (SO2) Database Long-Term L4 Global V2, Goddard Earth Sci. Data Inf. Serv. Cent. (GES DISC), doi:10.5067/MEASURES/SO2/DATA406, accessed: 29 October 2024.

Friedman, J. H.: Greedy Function Approximation: A Gradient Boosting Machine, Ann. Stat., 29, 1189–1232, http://www.jstor.org/stable/2699986, 2001.

Hersbach, H., Bell, B., Berrisford, P., Hirahara, S., Horányi, A., Muñoz-Sabater, J., Nicolas, J., Peubey, C., Radu, R., Schepers, D., Simmons, A., Soci, C., Abdalla, S., Abellan, X., Balsamo, G., Bechtold, P., Biavati, G., Bidlot, J., Bonavita, M., De Chiara, G., Dahlgren, P., Dee, D., Diamantakis, M., Dragani, R., Flemming, J., Forbes, R., Fuentes, M., Geer, A., Haimberger, L., Healy, S., Hogan, R. J., Hólm, E., Janisková, M., Keeley, S., Laloyaux, P., Lopez, P., Lupu, C., Radnoti, G., de Rosnay, P., Rozum, I., Vamborg, F., Villaume, S., and Thépaut, J.-N.: The ERA5 global reanalysis, Q. J. R. Meteorol. Soc., 146, 1999–2049, doi:10.1002/qj.3803, 2020.

Hoesly, R. M., Smith, S. J., Feng, L., Klimont, Z., Janssens-Maenhout, G., Pitkanen, T., Seibert, J. J., Vu, L., Andres, R. J., Bolt, R. M., Bond, T. C., Dawidowski, L., Kholod, N., Kurokawa, J.-I., Li, M., Liu, L., Lu, Z., Moura, M. C. P., O'Rourke, P. R., and Zhang, Q.: Historical (1750–2014) anthropogenic emissions of reactive gases and aerosols from the Community Emissions Data System (CEDS), Geosci. Model Dev., 11, 369–408, doi:10.5194/gmd-11-369-2018, 2018.

Kang, Y., Choi, H., Im, J., Park, S., Shin, M., Song, C.-K., and Kim, S.: Estimation of surface-level NO2 and O3 concentrations using TROPOMI data and machine learning over East Asia, Environ. Pollut., 288, 117711, doi:10.1016/j.envpol.2021.117711, 2021.

Kerminen, V.-M., Chen, X., Vakkari, V., Petäjä, T., Kulmala, M., and Bianchi, F.: Atmospheric new particle formation and growth: review of field observations, Environ. Res. Lett., 13, 103003, doi:10.1088/1748-9326/aadf3c, 2018.

Kharol, S. K., McLinden, C. A., Sioris, C. E., Shephard, M. W., Fioletov, V., van Donkelaar, A., Philip, S., and Martin, R. V.: OMI satellite observations of decadal changes in ground-level sulfur dioxide over North America, Atmos. Chem. Phys., 17, 5921–5929, doi:10.5194/acp-17-5921-2017, 2017.

Krotkov, N. A., McClure, B., Dickerson, R. R., Carn, S. A., Li, C., Bhartia, P. K., Yang, K., Krueger, A. J., Li, Z., Levelt, P. F., Chen, H., Wang, P., and Lu, D.: Validation of SO2 retrievals from the Ozone Monitoring Instrument over NE China, J. Geophys. Res. Atmos., 113, D16S40, doi:10.1029/2007JD008818, 2008.

Krotkov, N. A., Li, C., and Leonard, P.: OMI/Aura Sulphur Dioxide (SO2) Total Column Daily L2 Global Gridded 0.125 degree x 0.125 degree V3, Goddard Earth Sci. Data Inf. Serv. Cent. (GES DISC), doi:10.5067/Aura/OMI/DATA2023, accessed: 03/10/2024, 2014.

Krzyzanowski, M., and Wojtyniak, B.: Ten-Year Mortality in a Sample of an Adult Population in Relation to Air Pollution, J. Epidemiol. Community Health, 36, 262–268, http://www.jstor.org/stable/25566349, 1992.

https://doi.org/10.5194/egusphere-2025-1735
Preprint. Discussion started: 25 April 2025

Lamsal, L. N., Martin, R. V., van Donkelaar, A., Steinbacher, M., Celarier, E. A., Bucsela, E., Dunlea, E. J., and Pinto, J. P.: Ground-level nitrogen dioxide concentrations inferred from the satellite-borne Ozone Monitoring Instrument, J. Geophys. Res., 113, D16308, doi:10.1029/2007JD009235, 2008.

Lee, C., Martin, R. V., van Donkelaar, A., Lee, H., Dickerson, R. R., Hains, J. C., Krotkov, N., Richter, A., Vinnikov, K., and Schwab, J. J.: SO2 emissions and lifetimes: Estimates from inverse modeling using in situ and global, space-based (SCIAMACHY and OMI) observations, J. Geophys. Res., 116, D06304, doi:10.1029/2010JD014758, 2011.

Lee, S.-H., Gordon, H., Yu, H., Lehtipalo, K., Haley, R., Li, Y., and Zhang, R.: New particle formation in the atmosphere: From molecular clusters to global climate, J. Geophys. Res. Atmos., 124, doi:10.1029/2018JD029356, 2019.

Levelt, P. F., van den Oord, G. H. J., Dobber, M. R., Mälkki, A., Visser, H., de Vries, J., Stammes, P., Lundell, J. O. V., and Saari, H.: The Ozone Monitoring Instrument, IEEE Trans. Geosci. Remote Sens., 44, 1093–1101, doi:10.1109/TGRS.2006.872333, 2006.

Li, C., Joiner, J., Krotkov, N. A., and Bhartia, P. K.: A fast and sensitive new satellite SO2 retrieval algorithm based on principal component analysis: Application to the ozone monitoring instrument, Geophys. Res. Lett., 40, 6314–6318, doi:10.1002/2013GL058134, 2013.

Li, C., McLinden, C., Fioletov, V., Krotkov, N., Carn, S., Joiner, J., Streets, D., He, H., Ren, X., Li, Z., and Dickerson, R. R.: India Is Overtaking China as the World's Largest Emitter of Anthropogenic Sulfur Dioxide, Sci. Rep., 7, 14304, doi:10.1038/s41598-017-14639-8, 2017.

Li, C., Krotkov, N. A., Leonard, P. J. T., Carn, S., Joiner, J., Spurr, R. J. D., and Vasilkov, A.: Version 2 Ozone Monitoring Instrument SO2 product (OMSO2 V2): New anthropogenic SO2 vertical column density dataset, Atmos. Meas. Tech., 13, 6175–6191, doi:10.5194/amt-13-6175-2020, 2020a.

Li, C., Krotkov, N. A., Leonard, P., and Joiner, J.: OMI/Aura Sulphur Dioxide (SO2) Total Column 1-orbit L2 Swath 13x24 km V003, Goddard Earth Sci. Data Inf. Serv. Cent. (GES DISC), doi:10.5067/Aura/OMI/DATA2022, accessed: 29 October 2024, 2020b.

Liu, Y., Park, R. J., Jacob, D. J., Li, Q., Kilaru, V., and Sarnat, J. A.: Mapping annual mean ground-level PM2.5 concentrations using Multiangle Imaging Spectroradiometer aerosol optical thickness over the contiguous United States, J. Geophys. Res., 109, D22206, doi:10.1029/2004JD005025, 2004.

Lucchesi, R.: File Specification for GEOS FP, GMAO Office Note No. 4, Version 1.2, 61 pp., available at http://gmao.gsfc.nasa.gov/pubs/office_notes, 2018.

McLinden, C. A., Fioletov, V., Boersma, K. F., Kharol, S. K., Krotkov, N., Lamsal, L., Makar, P. A., Martin, R. V., Veefkind, J. P., and Yang, K.: Improved satellite retrievals of NO2 and SO2 over the Canadian oil sands and comparisons with surface measurements, Atmos. Chem. Phys., 14, 3637–3656, doi:10.5194/acp-14-3637-2014, 2014.

National Academy of Sciences, Engineering, and Medicine (NASEM): The Future of Atmospheric Chemistry Research: Remembering Yesterday, Understanding Today, Anticipating Tomorrow, Washington, DC, The National Academies Press, doi:10.17226/23573, 2016.

https://doi.org/10.5194/egusphere-2025-1735
Preprint. Discussion started: 25 April 2025

National Aeronautics and Space Administration (NASA): README Document for OMSO2: Aura/OMI Sulfur Dioxide Level 2 Product, Goddard Earth Sciences Data and Information Services Center (GES DISC), available at https://aura.gesdisc.eosdis.nasa.gov/data/Aura_OMI_Level2/OMSO2.003/doc/OMSO2Readme_V2.pdf, 2020.

Nowlan, C. R., Liu, X., Chance, K., Cai, Z., Kurosu, T. P., Lee, C., and Martin, R. V.: Retrievals of sulfur dioxide from the Global Ozone Monitoring Experiment 2 (GOME-2) using an optimal estimation approach: Algorithm and initial validation, J. Geophys. Res., 116, D18301, doi:10.1029/2011JD015808, 2011.

Philip, S., Martin, R. V., and Keller, C. A.: Sensitivity of chemistry-transport model simulations to the duration of chemical and transport operators: A case study with GEOS-Chem v10-01, Geosci. Model Dev., 9, 1683–1695, doi:10.5194/gmd-9-1683-2016, 2016.

Seinfeld, J. H., and Pandis, S. N. (3rd Ed.): Atmospheric Chemistry and Physics: From Air Pollution to Climate Change, Wiley, Hoboken, New Jersey, United States, 874-876, ISBN 9781118947401, 2016.

Veefkind, J. P., Aben, I., McMullan, K., Förster, H., de Vries, J., Otter, G., Claas, J., Eskes, H. J., de Haan, J. F., Kleipool, Q., van Weele, M., Hasekamp, O., Hoogeveen, R., Landgraf, J., Snel, R., Tol, P., Ingmann, P., Voors, R., Kruizinga, B., Vink, R., Visser, H., and Levelt, P. F.: TROPOMI on the ESA Sentinel-5 Precursor: A GMES mission for global observations of the atmospheric composition for climate, air quality, and ozone layer applications, Remote Sens. Environ., 120, 70–83, doi:10.1016/j.rse.2011.09.027, 2012.

Theys, N., De Smelt, I., van Gent, J., Danckaert, T., Wang, T., Hendrick, F., Stavrakou, T., Bauduin, S., Clarisse, L., Li, C., Krotkov, N., Yu, H., Brenot, H., and Van Roozendael, M.: Sulfur dioxide vertical column DOAS retrievals from the Ozone Monitoring Instrument: Global observations and comparison to ground-based and satellite data, J. Geophys. Res. Atmos., 120, 2470–2491, doi:10.1002/2014JD022657, 2015.

Wang, Y. and Wang, J.: Tropospheric SO2 and NO2 in 2012-2018: Contrasting views of two sensors (OMI and OMPS) from space, Atmospheric Environment, 223, 117214, doi:10.1016/j.atmosenv.2019.117214, 2020a.

Wang, Y., Wang, J., Xu, X., Henze, D. K., Qu, Z., and Yang, K.: Inverse modeling of SO2 and NOx emissions over China using multisensory satellite data – Part 1: Formulation and sensitivity analysis, Atmos. Chem. Phys., 20, 6631-6650, doi:10.5194/acp-20-6631-2020, 2020b

Wang, Y., Wang, J., Zhou, M., Henze, D. K., Ge, C., and Wang, W.: Inverse modeling of SO2 and NOx emissions over China using multisensory satellite data – Part 2: Downscaling techniques for air quality analysis and forecasts, Atmos. Chem. Phys., 20, 6651–6670, doi:10.5194/acp-20-6651-2020, 2020c.

Wei, J., Li, Z., Wang, J., Li, C., Gupta, P., and Cribb, M.: Ground-level gaseous pollutants (NO2, SO2, and CO) in China: Daily seamless mapping and spatiotemporal variations, Atmos. Chem. Phys., 23, 1511–1532, doi:10.5194/acp-23-1511-2023, 2023.

Yang, Q., Kim, J., Cho, Y., Lee, W.-J., Lee, D.-W., Yuan, Q., Wang, F., Zhou, C., Zhang, X., Xiao, X., Guo, M., Guo, Y., Carmichael, G. R., and Gao, M.: A synchronized estimation of hourly surface concentrations of six criteria air pollutants with GEMS data, npj Clim. Atmos. Sci., 6, 94, doi:10.1038/s41612-023-00407-1, 2023a.

https://doi.org/10.5194/egusphere-2025-1735
Preprint. Discussion started: 25 April 2025

Yang, Q., Yuan, Q., Gao, M., and Li, T.: A new perspective to satellite-based retrieval of ground-level air pollution: Simultaneous estimation of multiple pollutants based on physics-informed multi-task learning, Sci. Total Environ., 857, 159542, doi:10.1016/j.scitotenv.2022.159542, 2023b.

Zhang, S., Mi, T., Wu, Q., Luo, Y., Grieneisen, M. L., Shi, G., Yang, F., and Zhan, Y.: A data-augmentation approach to deriving long-term surface SO2 across Northern China: Implications for interpretable machine learning, Sci. Total Environ., 827, 154278, doi:10.1016/j.scitotenv.2022.154278, 2022.

Zhang, X., Wang, Z., Cheng, M., Wu, X., Zhan, N., and Xu, J.: Long-term ambient SO2 concentration and its exposure risk across China inferred from OMI observations from 2005 to 2018, Atmos. Res., 247, 105150, doi:10.1016/j.atmosres.2020.105150, 2021.

Zoogman, P., Liu, X., Suleiman, R. M., Pennington, W. F., Flittner, D. E., Al-Saadi, J. A., Hilton, B. B., Nicks, D. K., Newchurch, M. J., Carr, J. L., Janz, S. J., Andraschko, M. R., Arola, A., Baker, B. D., Canova, B. P., Chan Miller, C., Cohen, R. C., Davis, J. E., Dussault, M. E., Edwards, D. P., Fishman, J., Ghulam, A., González Abad, G., Grutter, M., Herman, J. R., Houck, J., Jacob, D. J., Joiner, J., Kerridge, B. J., Kim, J., Krotkov, N. A., Lamsal, L., Li, C., Lindfors, A., Martin, R. V., McElroy, C. T., McLinden, C., Natraj, V., Neil, D. O., Nowlan, C. R., O'Sullivan, E. J., Palmer, P. I., Pierce, R. B., Pippin, M. R., Saiz-Lopez, A., Spurr, R. J. D., Szykman, J. J., Torres, O., Veefkind, J. P., Veihelmann, B., Wang, H., Wang, J., and Chance, K.: Tropospheric emissions: Monitoring of pollution (TEMPO), J. Quant. Spectrosc. Radiat. Transf., 186, 17–39, doi:10.1016/j.jqsrt.2016.05.008, 2017.